Chemical Engineering Journal 427 (2022) 130889

Contents lists available at ScienceDirect

Chemical Engineering Journal

journal homepage: www.elsevier.com/locate/cej

Efficient Solid-State triplet-triplet annihilation up-conversion electroluminescence device by incorporating intermolecular intersystem-crossing dark sensitizer

Chia-Hsun Chen [a], Bo-Yen Lin [b], Nathan T. Tierce [c], Man-kit Leung [a], Tien-Lung Chiu [b,*], Christopher J. Bardeen [c,*], Jiun-Haw Lee [d,*]

[a] Department of Chemistry, National Taiwan University, Taiwan
[b] Department of Electrical Engineering, Yuan Ze University, Taiwan
[c] Department of Chemistry, University of California, Riverside, United States
[d] Graduate Institute of Photonics and Optoelectronics and Department of Electrical Engineering, National Taiwan University, Taiwan

ARTICLE INFO

Keywords:
Dark sensitizer triplet–triplet annihilation upconversion (DS-TTAUC)
intersystem crossing (ISC)
organic light emitting diode (OLED)

ABSTRACT

The efficient conversion of electron-hole (e-h) pairs into triplet excitons is a challenge for blue organic light-emitting diodes (OLEDs) based on triplet–triplet annihilation upconversion (TTAUC). The 25% fraction of e-h pairs that create singlet excitons represents a significant loss channel that can lead to parasitic red-shifted emission. In this study, an intermolecular intersystem crossing that relies on a "dark sensitizer" (DS) layer consisting of tris-(8-hydroxyquinoline)aluminum (Alq_3) doped with tris[2-phenylpyridinato-C2,N]Iridium(III) ($Ir(ppy)_3$) is demonstrated to enhance the TTAUC process. Carriers recombination and excitons generation are formed on Alq_3 molecules. Alq_3 singlet excitons are then quenched by the $Ir(ppy)_3$ triplet state, followed by energy transfer to the Alq_3 triplet state. The non-emissive, long-lived Alq_3 triplets migrate from the sensitizer layer to an emitter layer where they undergo TTAUC to give blue fluorescence emission. This DS-TTAUC process promises no green emission from the Alq_3. The efficiency of a blue OLED utilizing DS-TTAUC was improved by 34.2% compared to a standard TTAUC OLED. In addition, the device exhibited CIE coordinates of (0.15, 0.09). Furthermore, a high photoluminescence quantum yield fluorescence emitter is incorporated to enhance the singlet exciton emission in the emitter layer. A maximum external quantum efficiency of 7.54% can be achieved with recorded-high quantum yield of the TTAUC (Φ_{TTAUC}) = 37.6% in solid state.

1. Introduction

Triplet-triplet annihilation upconversion (TTAUC) is a nonlinear process that converts two low-energy triplet excitons into a single high energy photon as shown in Fig. 1**a** [1-5]. Triplet states can be created either optically using a sensitizer that creates a triplet state via intersystem crossing (ISC) or by electrical pumping via e-h recombination. In both cases, the upconversion happens when two triplets fuse (annihilate) to leave the emitter in its higher energy singlet state, where it emits a higher energy photon. TTAUC is an attractive strategy for blue-emitting OLED devices, since electron-hole (e-h) recombination yields 75% triplet excitons by spin statistics, providing an efficient way to generate triplet states and allow the use of a lower driving voltage for electrofluorescence [6,7]. In addition, the triplet energy migration and diffusion play a curial role to determine the triplet energy transfer (TET) and TTAUC ability, as well as the device efficiency performances. The material aggregation and self-assembly with well molecular packing strengthen the triplet energy migration and diffusion, which is beneficial for the efficiency of TTAUC system [5,8,9]. For example, N. Yanai and N. Kimizuka reported a review on triplet energy migration-based UC (TEM-UC) to achieve high-efficiency TTAUC performances [5].

In using a TTAUC scheme in an OLED, where e-h recombination produces the low-energy triplets, there are several challenges. The first challenge is finding a combination of materials that not only have the correct singlet and triplet energy level alignments but also support good carrier transport. The second challenge is to prevent the high energy singlet state from being quenched by the low energy sensitizer. In fluid media that permit molecular diffusion (liquids, gels, elastomers), the

* Corresponding authors.
E-mail addresses: tlchiu@saturn.yzu.edu.tw (T.-L. Chiu), christob@ucr.edu (C.J. Bardeen), jiunhawlee@ntu.edu.tw (J.-H. Lee).

https://doi.org/10.1016/j.cej.2021.130889
Received 15 March 2021; Received in revised form 4 June 2021; Accepted 15 June 2021
Available online 18 June 2021

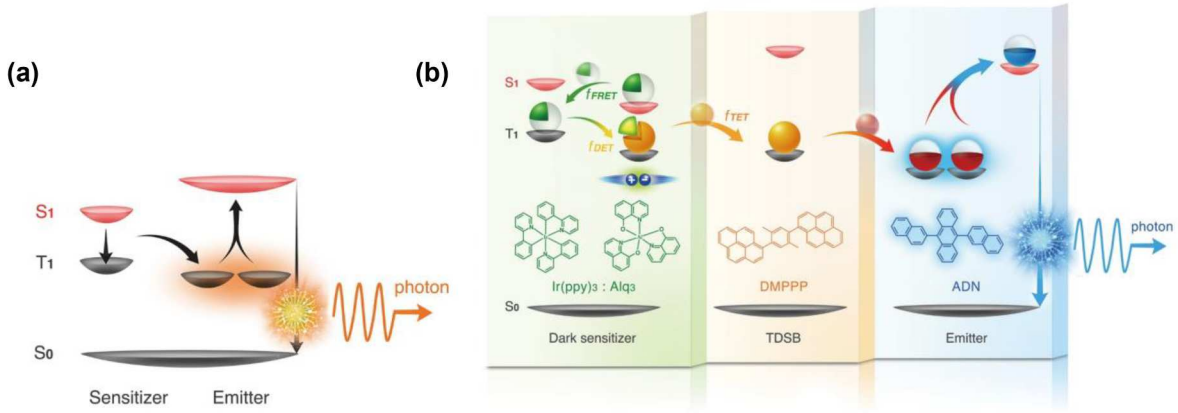

Fig. 1. (a) Energy transfer of conventional TTAUC process from the singlet state of sensitizer to the singlet state of emitter. (b) Energy levels of DS-TTAUC trilayer structure and their molecular structures applied for dark sensitizer, TDSB, and emitter layers. When OLED is lit-on, DS-TTAUC energy transfer is illustrated starting from the carrier recombination to photon emission.

sensitizer can spatially separate from the emitter before the high energy singlet state is created by TTA. In rigid films, spatial proximity of sensitizer and emitter often results in singlet quenching of high-energy emitter by low-energy sensitizer. We recently reported an exciplex sensitizer for TTAUC to observe the blue emission with a low driving voltage of 2.2 V [10]. We also employed tris-(8-hydroxyquinoline) aluminum (Alq_3), a well-established OLED material with favorable processability and stability, as sensitizer for efficient TTAUC [11]. When the Alq_3 sensitizer was combined with a TTA emitter (9,10-bis(2′-naphthyl) anthracene (ADN)) and a triplet-diffusion-singlet-blocking (TDSB) layer composed of 1-(2,5-dimethyl-4-(1-pyrenyl)phenyl) pyrene (DMPPP), a high intrinsic efficiency of the used triplets by TTAUC (η_{TTAUC} = 86.1%) was achieved, accompanied by improved device efficiency. The theoretical internal quantum efficiency (IQE) of TTAUC-OLED is 50%, which is so-called the overall quantum yield of the emitted photons by TTAUC (Φ_{TTAUC}) in this study. Although this IQE value is much lower than the theoretical 100% IQE of phosphorescence and thermal activated delayed fluorescence (TADF) OLEDs, TTAUC-OLEDs have a great advantage in the low driving voltage and power efficiency (PE) because the high-energy emission photons (e.g. blue one ~ 3 eV) are launched by low-energy triplets (e.g. E_T ~ 1.7 eV). Moreover, this trilayer TTAUC-OLEDs have a great potential to reduce the triplet-polaron quenching (TPQ) by spatially separating the carrier recombination and photon emission zone, which may result in the greater PE at high current density region, longer device operation lifetime and larger triplet contributions comparing to conventional TTA-OLED [12]. In addition, the robust sensitizer profits to the device stability and long operational lifetime of blue OLED. However, the blue OLED performance was still limited by residual green emission from the Alq_3, originating from the 25% yield of singlet excitons from e-h recombination.

In a TTAUC OLED, the goal is to shift the e-h recombination yield to 100% triplet excitons. However, just as in a traditional OLED, spin statistics present a challenge. To drive the triplet yield to 100%, a standard chemical strategy would be to utilize the heavy atom effect to enhance intramolecular spin–orbit coupling and promote ISC. This source of spin–orbit coupling relies on orbital overlap and requires close contact between atom and molecule to accelerate all singlet–triplet relaxation processes, both $S_1 \rightarrow T_1$ and $T_1 \rightarrow S_0$. The presence of a heavy atom, typically a metal ion, would also introduce undesired charge recombination centers into the organic. In this paper, we adopt a new approach that relies on intermolecular ISC, a phenomenon that was identified decades ago but that has not been exploited in the organic electronics field [13-15]. Tris[2-phenylpyridinato-C2,N]Iridium(III) ($Ir(ppy)_3$) incorporated into the fluorescent Alq_3 recombination layer can act as a "dark sensitizer" (DS) because the $Ir(ppy)_3$ effectively quenches the Alq_3 singlet and transfers its energy to the Alq_3 triplet. In the DS approach, ISC is promoted by intermolecular energy transfer that can act over long distances to populate an intermediate state with mixed singlet/triplet character that can enhance the overall $S_1 \rightarrow T_1$ ISC relaxation in Alq_3.

In this paper, we demonstrate that by using the DS concept, the external quantum efficiency (EQE) of blue TTAUC OLEDs can be increased by 34.2% compared to a device using only an Alq_3 sensitizer layer. Nearly 100% ISC efficiency from the Alq_3 singlet to its triplet state is obtained, allowing the device to fully utilize the triplet excitons produced by electrical pumping [16-18]. The remaining emission from both Alq_3 and $Ir(ppy)_3$ was almost completely eliminated, so the color performance is almost identical in CIE coordinates to that of a blue TTA OLED using only a single ADN layer. Finally, a high efficiency DS-TTAUC OLED was demonstrated by replacing the ADN layer with one that incorporates a high photoluminescence quantum yield (PLQY) blue naphthalene indenofluorene core dopant (DPaNIF) in an anthracene-based TTA host (NPAN). The combined use of the DS layer to harvest triplets, a TDSB layer to transfer them, and an optimized emitter layer yielded a blue TTAUC OLED with an EQE of 7.54%.

2. Experimental section

ITO coated glass substrates were first treated by an O_2 plasma (PDC-32G) and then placed into a thermal evaporator. All the layers including the metal cathode were deposited under high vacuum (5×10^{-6} torr). 1 Å/s deposition rate was used for organic layers, and 10 Å/s for aluminum. After deposition, devices were transferred into a N_2 glove box and encapsulated with a cover glass using a UV-curing epoxy resin. In order to accelerate the device aging, the device packaged without containing moisture-particle getter. Characteristics of the OLEDs were measured by a spectrometer (Minolta CS-1000) with a source meter (Keithley 2400). The setup for time-resolved electroluminescence (TrEL) consisted of a function generator (Agilent 33500B), a source meter (Keithley 2400), a photomultiplier (PMT, Hamamatsu H6780-20) and an oscilloscope (Tektronix TDS2004C). To separate the contribution from blue and green emissions, 450-nm short pass (Thorlabs FESH0450) and 600-nm long pass (Thorlabs FEL0600) filters were placed in the beam path.

The time-resolved PL (TRPL) setup was based on a Coherent Libra regeneratively amplified Ti: Sapphire laser system operating at 1 kHz repetition rate that generated 200 fs pulses at 800 nm. The 800-nm output was frequency doubled to 400 nm using a Type I BBO crystal. The sample photoluminescence was detected using a monochromator coupled to a picosecond streak camera (Hamamatsu C4334 Streakscope). A 420-nm long pass filter was placed in front of the streak camera to filter out the excitation laser. The signal was recorded by the

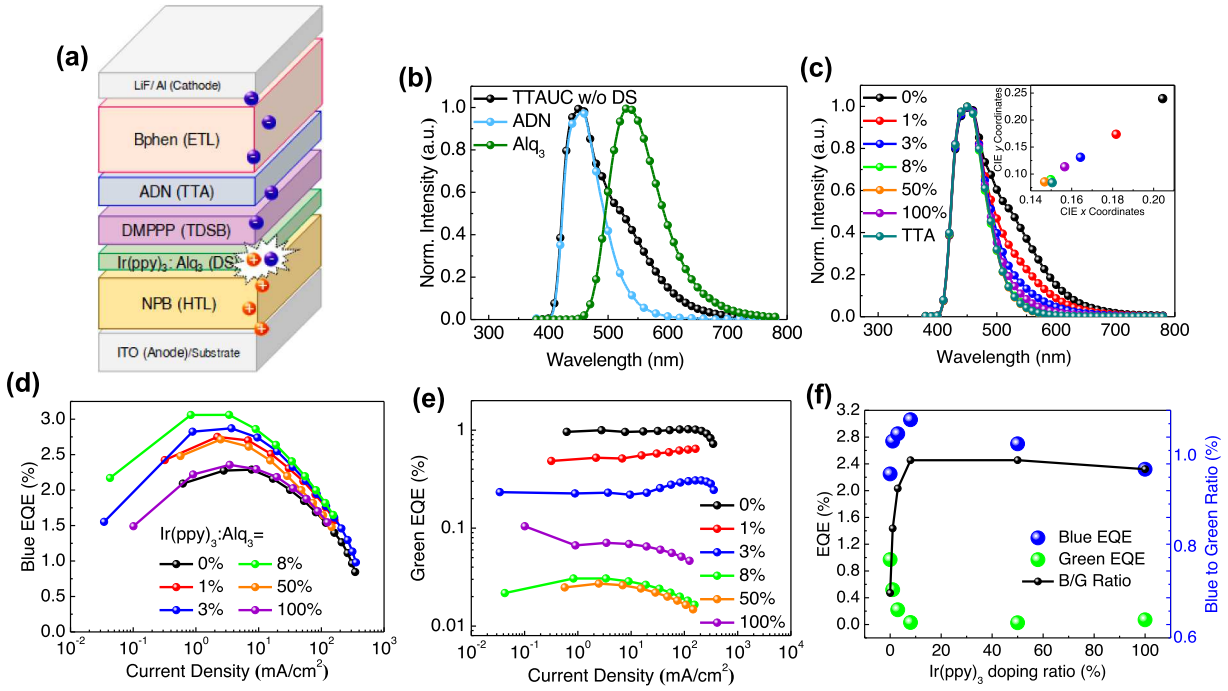

Fig. 2. (a) Device structure. (b) EL Spectra of TTAUC OLED with 0% $Ir(ppy)_3$ and OLEDs with Alq_3 and ADN emitters and (c) EL spectra for TTAUC OLEDs at 9 mA/cm^2 with various $Ir(ppy)_3$ concentration. Inset of (c) shows CIE coordination of devices. (d) Blue and (e) green EQE versus current density. (f) Blue-to-green ratio and EQE.

streak camera as a two-dimensional data matrix including time and wavelength with resolutions of 25 ps and 2.5 nm, respectively. A Stanford Research Systems DG535 pulse generator was used to delay the laser pulse for scans longer than 1 μs. The setup of PL quantum yield measurement consisted of a Xenon lamp and monochromator (Horiba, iHR320) as a light source while the sample signal was collected by a photomultiplier tube (PMT). The η_{PLQY} was measured by using integrating sphere (Quanta-φ manual Rev C F-3029) as sample holder and calculated by software (FluorEssence).

3. Results and discussions

3.1. Schematic of energy level and energy transfer

The energy level diagram for the DS-TTAUC trilayer device is shown in Fig. 1**b**. The $Ir(ppy)_3$:Alq_3, DMPPP and ADN serve as the dark sensitizer, TDSB and TTA emitter layers, respectively. Their molecular structures and energy levels are illustrated in Fig. 1**b** and **Fig. S1** (see Supplementary Information), respectively. For efficient TTAUC process (as **Fig. S2**), the TDSB layer was necessary and inserted between sensitizer and emitter layers to prevent ADN singlet quenching by the Ir $(ppy)_3$:Alq_3 layer while maintaining a triplet diffusion route from sensitizer to emitter [19,20]. The requirement for TDSB layer should have no TTA or any upconversion ability to prevent the energy loss. In this study, DMPPP was chosen as the TDSB material without TTA capability [21]. In general, this sensitizer strategy is universal for various sensitizer composition (such as perovskite and its quantum dot [22], TADF and phosphorescence (**Fig. S3**)) to exhibit the efficient TET and TTAUC processes, corresponding to the efficient electroluminescence devices. In **Fig. S3**, the case $Ir(ppy)_3$:Alq_3 sensitizer shows the highest intensity and pure blue emission, which indicates the high-efficiency TET and TTAUC processes. Hence, the following discussion is focusing on this case. The singlet and triplet levels of Alq_3 are located at 2.7 and 2.0 eV, respectively. $Ir(ppy)_3$, with singlet and triplet energies of 2.8 and 2.4 eV respectively, was doped into Alq_3 to form the DS layer. Note that the metal-to-ligand charge transfer state (^{1}MLCT) absorption of $Ir(ppy)_3$ does not overlap with the Alq_3 emission, so population transfer to the singlet level of $Ir(ppy)_3$ can be neglected. The ^{3}MLCT absorption spectrum of $Ir(ppy)_3$ overlaps with the emission spectrum of Alq_3 singlet, allowing Förster resonance energy transfer (FRET) from the Alq_3 S_1 state to the $Ir(ppy)_3$ T_1 state with efficiency f_{FRET}. Note that the S_0-T_1 transition of $Ir(ppy)_3$ normally would be spin-forbidden but strong spin–orbit coupling provides it with appreciable oscillator strength. The Alq_3 T_1 state then acts as a triplet quencher for the $Ir(ppy)_3$ T_1 state, most likely through Dexter energy transfer with efficiency f_{DET}. In summary, a singlet from Alq_3 can efficiently transfer its energy to its triplet state through a $Ir(ppy)_3$ triplet state intermediate, providing an intermolecular ISC channel for Alq_3.

3.2. Electroluminescent performances of DS-TTAUC OLEDs.

In conventional phosphorescent OLEDs, a wide bandgap material, such as 4,4′-bis(N-carbazolyl)-1,1′-biphenyl (CBP), is typically used as a host for $Ir(ppy)_3$ [23]. $Ir(ppy)_3$ doped Alq_3 thin films have only been used as a purpose to probe the phosphorescence for Alq_3 in low-temperature photoluminescence measurements [24-27]. For this DS-TTAUC OLED, the device structure (Fig. 2**a**) is ITO / *N,N'* diphenyl-*N, N'*-bis(1-napthyl)-1,1′-biphenyl-4,4′-diamine (NPB, 50 nm)/ $Ir(ppy)_3$: Alq_3 (5 nm)/ DMPPP (10 nm)/ ADN (10 nm)/ bathophenanthroline (Bphen, 65 nm)/ lithium fluoride (LiF, 0.8 nm)/ aluminum (Al, 100 nm), where ITO is anode, NPB is hole transporting layer (HTL), $Ir(ppy)_3$: Alq_3 is dark sensitizer (DS) layer, DMPPP is triplet-diffusion-singlet-blocking (TDSB) layer, ADN is TTA emitting layer (EML), BPhen is electron transporting layer (ETL), LiF is electron injection layer, and Al is cathode. Trilayer structure of the EML aims to separate the carrier recombination and photon emission zone, which reduces the TPQ, instead of mixing them into one layer [18]. The thickness of DMPPP in this study is set to 10 nm, based on the optimization of monitoring maximum blue EQEs (**Fig. S4**).

The EL spectra of TTAUC OLED with a TDSB layer (device structure of ITO/ NPB (50 nm)/ Alq_3 (5 nm)/ DMPPP (10 nm)/ ADN (10 nm)/ Bphen (65 nm)/ LiF/ Al) is shown in Fig. 2**b**. For comparison, two OLEDs

Table 1
EQE performance of TTAUC OLED with various $Ir(ppy)_3$ doping concentrations at J = 3 mA/cm^2, which around their maximum values. Blue and green emission were separated from the EL spectra. Prompt and delayed fluorescence were separated using TrEL. Blue and green EQEs were separated from EL spectra.

Doping	EQE (Total)	EQE (Blue)		EQE (Green)	
		Prompt	Delayed	Prompt	Delayed
0%	3.26%	0%	2.28%	0.892%	0.077%
1%	3.26%		2.75%	0.488%	0.031%
3%	3.10%		2.87%	0.191%	0.028%
8%	3.09%		3.06%	0.016%	0.013%
50%	2.73%		2.71%	0.000%	0.026%
100%	2.42%		2.35%	0.049%	0.021%

with structure of ITO/ NPB (50 nm)/ Alq3 (5 nm)/ Bphen (65 nm)/ LiF/ Al and ITO/ NPB (50 nm)/ ADN (10 nm)/ Bphen (65 nm)/ LiF/ Al were fabricated to provide the pure Alq_3 and ADN EL spectra. The emission of the TTAUC OLED consists of both green Alq_3 (peak at 534 nm) and blue ADN (peak at 454 nm) contributions. Here, the sensitizer (pure Alq_3) was not "dark" and contributed to green emission. As shown in Fig. 2**c**, incorporation of $Ir(ppy)_3$ concentration (from 1% to 100%) in the Alq_3 matrix, EL spectra exhibits a decrease in green emission between 500 and 600 nm. Except for pure $Ir(ppy)_3$ case, these devices show almost identical J-V characteristics, and divergent L-V characteristics (see **Fig. S5**). The identical J-V behaviors indicated that the carrier transportation and recombination were mainly relied on the Alq_3 molecules rather than $Ir(ppy)_3$ molecules. The divergent L-V behaviors were resulted from different TET abilities of these DS layers. When the mass fraction of $Ir(ppy)_3$ was between 8% and 50%, the EL spectra almost overlapped with ADN-based TTA OLED, i.e. pure blue emission. As shown in inset of Fig. 2**c**, the CIE coordinates of the TTAUC OLED with doping ratios 8–50% were close to those of an ADN only device. Fig. 2**d and 2e** show the TTAUC-OLED EQEs separated into blue and green contributions based on the EL emission profiles of ADN- and Alq_3-based OLEDs shown in Fig. 2**b**. As the $Ir(ppy)_3$ doping ratio increased from 0% to 8%, the blue EQE increased from 2.28% to 3.06% while the intensity of the green (sensitizer) emission was reduced by a factor of 50 (Table 1). At higher $Ir(ppy)_3$ ratios (50%), the blue EQE decreased while the green EQE reached its minimum value. At 100% $Ir(ppy)_3$, the blue contribution decreased to 2.35% and a green emission from $Ir(ppy)_3$ reappeared. The blue-to-green ratio for EL device achieved its highest value when the $Ir(ppy)_3$ doping ratio was 8%, as seen in Fig. 2**f**. Table 1 summarizes the EQE performance of each device. In addition, these TTAUC devices take place the efficiency roll-off in high current density regimes due to TPQ, especially in TTA blue EQE (Fig. 2**d**). Although the high triplet density in high current density regime is good for generating TTA photon, the polaron density is also high to make TPQ happen easily, which leads the efficiency roll-off.

3.3. TrEL characteristics

The physical origins of the blue and green emission components can be clarified using TrEL measurements. The total EQE values in Table 1 can be separated into prompt and delayed components using time-resolved measurements. A 450-nm short-pass and a 600-nm long-pass filters were used to separate the blue and green contributions on EQE as the spectra in Fig. 2**b**. The Alq_3 spectrum reached to 700 nm, which was used to evaluate the contribution from Alq_3 green emission through the 600-nm long-pass filter. The contribution from ADN emission was deduced using the 450-nm short-pass filter. Fig. 3**a** shows the TrEL measurements for the blue emission in DS-TTAUC OLED (the detail TrEL results see **Fig. S6–S8**). A shortpass filter (λ less than 450 nm) was employed to filter out Alq_3 emission. The microsecond TrEL of the blue emission for all doping ratios showed a single decayed signal, which indicates that all the blue photons came from TTA originating from the long-lived triplet state of ADN, not from the carrier recombination at ADN or DMPPP layer. Without prompt fluorescence behavior of the TrEL signal, the major carrier recombination zone was affirmed to locate at the DS layer, and then the generated excitons energy transferred to be ADN emission because of the aforementioned TTAUC process. In addition, a reversed bias (-6 V) was applied on the device during the TrEL measurement to evaluate the carrier trapping effect by extracting the carriers back to their original electrodes. The identical TrEL signals was obtained indicating no concern on carrier trapping effect. The green EQEs with prompt and delayed contributions are summarized in Table 1. As the $Ir(ppy)_3$ doping ratio increased, the prompt TrEL of green emission originating from the Alq_3 singlet state decreased as shown in Fig. 3**b**, indicating efficient energy transfer from Alq_3 to $Ir(ppy)_3$, and achieved its lowest value for 8% doping. Note that a little delayed component of green emission was observed due to energy transfer from the high-energy TTAUC excitons back to the low-bandgap DS materials. At low doping concentrations (0–8%), the delayed components of the green EQE (ranging from 0.077% to 0.013%) come from singlet energy back transfer from the ADN S_1 to the Alq_3 S_1. On the other hand, the delayed green components (ranging from 0.026% to 0.021%) of the heavy doping cases (50% and 100%) describe that the singlet energy back transfer from the ADN S_1 to the $Ir(ppy)_3$ T_1. The DMPPP insertion layer reduced this singlet quenching effect on ADN but did not completely eliminate it. For the pure $Ir(ppy)_3$ case (100%), a decrease in the prompt signal may result from concentration quenching of $Ir(ppy)_3$. Fig. 3**c** shows the normalized TrEL of the blue component for DS-TTAUC OLED with 8% $Ir(ppy)_3$ under different driving voltages. As the driving voltages increased, the lifetime of the delayed EL decreased (see **Fig. S7g**) because TPQ happened when electrons transported through the ADN layer.

3.4. TRPL characteristics

The key to the improved performance of the DS-TTAUC OLED is the efficient harvesting of singlet excitons formed in the Alq_3 layer. In order

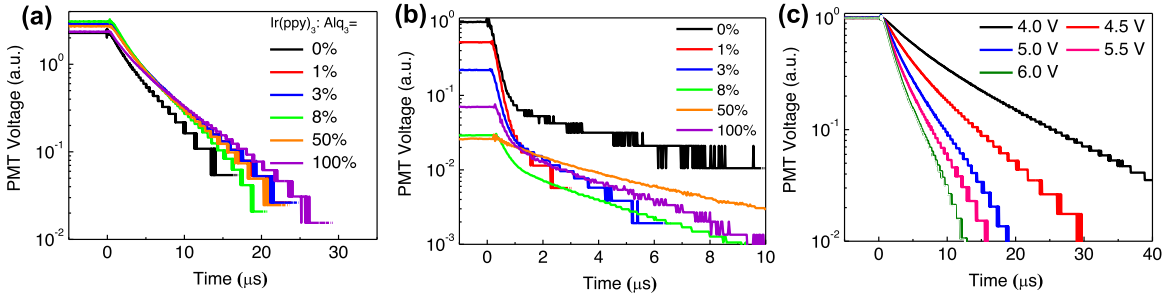

Fig. 3. TrEL of (a) blue and (b) green component of DS-TTAUC OLED with TDSB layer under various doping concentration at 5.0 V and (c) Normalized TrEL of blue component.

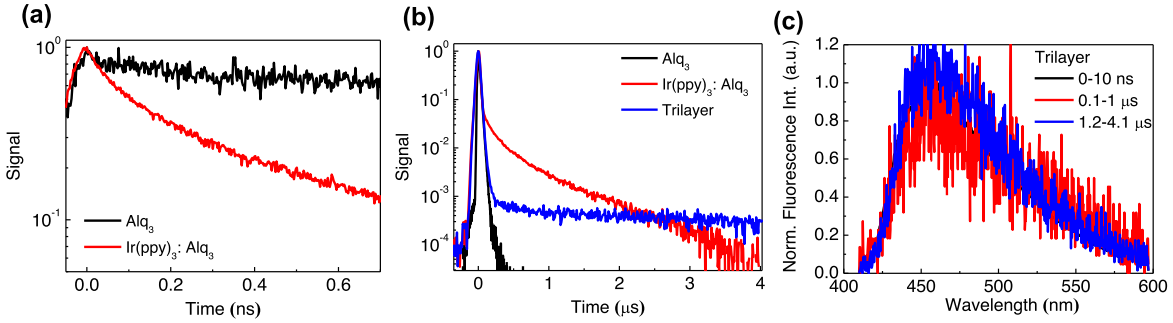

Fig. 4. Fluorescence decay at (a) short, and (b) long time window. (c) TRPL spectra for trilayer film over three time windows: 0–10 ns, 0.1–1 μs and 1.2–4.1 μs.

to selectively probe the singlet dynamics, optical excitation was conducted to create an initial population of singlet excitons and monitor their dynamics using TRPL. As shown in Fig. 4**a**, the singlet lifetime of the Alq_3 thin film decreased from 16.8 to 0.2 ns with the introduction of 8% $Ir(ppy)_3$. From the rapid decay, the energy transfer rate $k_{AI}^{\rightarrow} = 4.9 \times 10^9\ s^{-1}$ can be estimated. In longer time windows, a nonexponential component from the $Ir(ppy)_3$ emission was observed with contribution less than 1%. This component likely reflects the small fraction of Ir $(ppy)_3$ dopant molecules that are directly excited by the 400 nm pulse but cannot undergo rapid TET to nearby Alq_3 molecules. TRPL experiments were also conducted on the trilayer structure 8% $Ir(ppy)_3$:Alq_3 (30 nm)/ DMPPP (10 nm)/ ADN (30 nm). The trilayer exhibited the dramatic bi-exponential decay shown in Fig. 4**b**. In addition to the rapid decay of the Alq_3 layer, there is now a component that is longer-lived than either $Ir(ppy)_3$ or Alq_3, which we assign to the TTAUC signal arising from triplets created in the DS layer. The TRPL spectra of the trilayer thin film for 0–10 ns, 0.1–1 μs and 1.2–4.1 μs time windows are shown in Fig. 4**c**. A blue emission spectrum similar to ADN was observed in all three time windows. The 0–0.7 ns emission is due to ADN molecules directly excited at 400 nm, but the since a neat ADN thin film has a PL lifetime shorter than 20 ns, the emission in later windows must arise from TTA. Because ISC and singlet fission are negligible for ADN, the source of these triplets must be the $Ir(ppy)_3$:Alq_3-sensitizer layer where they are rapidly created by intermolecular ISC.

With the ability of $Ir(ppy)_3$ to facilitate creation of Alq_3 triplets now established, the next question is how efficiently are they transferred across the TDSB layer to the ADN emitter layer. It is possible to estimate these efficiencies from the EQE measurements. The EQE of the blue signal from the TTAUC OLED can be defined as [18]:

$$EQE = \frac{f_{exciton} \times (f_{triplet} + f_{singlet} \times f_{FRET} \times f_{DET}) \times \eta_{TTAUC} \times \eta_{PLQY} \times f_{outcoupling}}{2} \quad (1)$$

$$\Phi_{TTAUC} = \frac{EQE_{TTAUC}}{f_{exciton} \times (f_{triplet} + f_{singlet}) \times f_{TET} \times f_{outcoupling}} \quad (2)$$

Equation (1) describes the "blue delayed EQE" listed in Table 1. In this equation, $f_{exciton}$ is the conversion efficiency from carriers to excitons in the sensitizer layer, which is assumed to be 1 in our case. $f_{singlet}$ and $f_{triplet}$ are the fraction of electron-hole pairs converted into singlet and triplet excitons of Alq_3 molecules and are assumed to be 25% and 75%, respectively. η_{PLQY} is the quantum yield of singlet emission from ADN, which is 33%. $f_{outcoupling}$ is the outcoupling efficiency, which is assumed to be 20%. η_{TTAUC} is the intrinsic efficiency of the used triplets by TTAUC in the ADN layer, which can be understood as the triplet number outputted through TTAUC mechanism divided by the input triplet number received from the TDSB layer [28]. Φ_{TTAUC} in Eq. (2) is overall quantum yield of the emitted photons that transferred from triplets to singlets by TTAUC mechanism. Obviously, η_{TTAUC} can be obtained by deriving from the Eq.1 and Eq. (2) to be $2\Phi_{TTAUC}/\eta_{PLQY}$. This describes the triplet outputted efficiency through TTAUC mechanism including the TTAUC-singlets even not become photon emission (depended on η_{PLQY}). Hence, the theoretical maximum limit of η_{TTAUC} and Φ_{TTAUC} are 100% and 50%, respectively. η_{TTAUC} is a constant for samples with various $Ir(ppy)_3$ concentrations. One can estimate this η_{TTAUC} value from the measured EQE with $Ir(ppy)_3$ = 0% and the assumed $f_{triplet}$ = 75%, f_{FRET} = 0%, and f_{DET} = 0%, respectively. Note that ISC of Alq_3 is negligible. η_{TTAUC} for this TTAUC OLED is calculates to be 92.1% (the efficiency of energy transfer from Alq_3 triplet to ADN singlet), which is the highest value ever reported to our best knowledge [18].

For the case with DS ($Ir(ppy)_3 \neq 0$), as shown in Fig. 4, the Alq_3 singlet state transfers energy to the $Ir(ppy)_3$ triplet though FRET with efficiency f_{FRET}. Then the $Ir(ppy)_3$ triplet transfers the energy back to the Alq_3 triplet with efficiency f_{DET}. By assuming $f_{DET} = 1$ at lower $Ir(ppy)_3$ concentrations ($\leq$8%), f_{FRET} can be estimated from the prompt green EQE values using the following Eq. (3).

$$f_F = \frac{\text{Prompt EQE}_{\text{Green}}(x\%)}{\text{Prompt EQE}_{\text{Green}}(0\%)} = \frac{k_{Radiative} + k_{Non-radiative}}{k_{Radiative} + k_{Non-radiative} + k_{FRET}} = 1 - \frac{k_{FRET}}{k_{Radiative} + k_{Non-radiative} + k_{FRET}} = 1 - f_{FRET} \quad (3)$$

Here f_F is Alq_3 fluorescence intensity ratio for the $Ir(ppy)_3$:Alq_3 divided by the pure Alq_3 case. $k_{Radiative}$ and $k_{Non\text{-}radiative}$ are the radiative and non-radiative decay rates of Alq_3 singlet, respectively. k_{FRET} is the FRET rate from Alq_3 singlet to $Ir(ppy)_3$ triplet. From Eq. (4), f_{FRET} can be estimated from the data in Table 1. The results are shown in **Table S2**. f_{FRET} increased with increasing $Ir(ppy)_3$ and achieved almost complete FRET (98%) with 8% $Ir(ppy)_3$ in Alq_3.

$$f_{FRET} = \frac{k_{FRET}}{k_{Radiative} + k_{Non-radiative} + k_{FRET}} = \frac{1}{1 + (\frac{R}{R_0})^6} \quad (4)$$

By using the f_{FRET} values in **Table S2**, along with $f_{DET} = 1$, η_{TTAUC} = 92.1%, and η_{PLQY} = 33%, the calculated EQE for the TTAUC OLEDs with dopant concentrations of 0, 1%, 3%, and 8% values agreed well with the experimental results, showing that the data from the TRPL and EQE measurements are self-consistent. At 8% doping, with $f_{FRET} \sim 1$ and f_{DET} = 1, all the 25% singlet excitons from Alq_3 are converted into triplets, leading to a 1.33-times ((25%+75%)/75%) improvement in the TTAUC emission relative to the ADN-only device. This improvement, close to the theoretical limit, shows that intermolecular ISC is a remarkably effective strategy for turning singlets into triplets without appreciable loss (**Table S2**).

3.5. Efficiency enhancement on DS-TTAUC OLED

Further efficiency improvement of the DS-TTAUC OLED is possible by introducing emitter materials with higher η_{TTAUC} and η_{PLQY} values. To demonstrate this capability, we replaced the ADN with a DPaNIF:NPAN mixed layer [29,30]. To enhance the radiative rate for TTAUC singlet exciton, the blue emitter DPaNIF (η_{PLQY} of 97.4%) was doped into the anthracene-based TTA host NPAN (η_{TTAUC} of 77.4%). The molecular

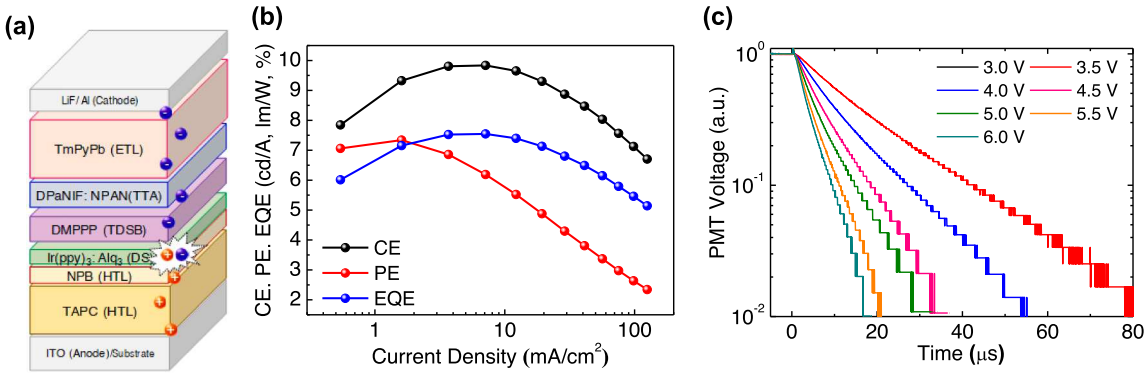

Fig. 5. (a) Device structure. (b) Current efficiency (CE), power efficiency (PE), external quantum efficiency (EQE) versus current density and (c) time-resolved EL of high efficiency DS-TTAUC OLED.

structures and photophysical properties of NPAN and DPaNIF are shown in **Fig. S9(a)**. The device structure of this high-efficiency DS-TTAUC OLED was ITO/ 1,1-bis[(di-4-tolylamino)phenyl]cyclohexane (TAPC, 40 nm)/ NPB (10 nm)/ Ir(ppy)$_3$: Alq$_3$ (5 nm)/ DMPPP (10 nm)/ DPaNIF: NPAN (12.5 nm, 3%)/ 1,3,5-tri(m-pyridin-3-ylphenyl)benzene (TmPyPb, 45 nm)/ LiF (0.8 nm)/ Al (100 nm), where TAPC and NPB are HTLs, DPaNIF: NPAN is TTA EML, TmPyPb is ETL, as shown in Fig. 5**a**. For this device, an EQE of 7.54% was obtained as shown in Fig. 5**b**. The exciton lifetime accelerated from 5.1 ns (NPAN film) to 3.2 ns (DPaNIF: NPAN mixed film) which is consistent with a higher radiative rate, which is promising as EML for high efficiency DS-TTAUC OLED. The highest current efficiency (CE), power efficiency (PE) and EQE reached 9.83 cd/A, 7.33 lm/W and 7.54%, respectively, with CIE coordinates of (0.13, 0.20). TrEL measurements in Fig. 5**c** show that all EL signals originated from delayed fluorescence without any prompt component, which confirmed the dominant contribution of triplet excitons via the TTAUC process. Using equation (1) and assuming an outcoupling efficiency ($f_{outcoupling}$) of 0.2, η_{PLQY} of 0.97, fraction of electron–hole pairs converted into triplet excitons ($f_{triplet} + f_{singlet}$) of 1 and exciton formation probability ($f_{exciton}$) of 1, the calculated η_{TTAUC} of the DS-TTAUC OLED decreased from 92.1% to 77.4%. This might attributed to the disruption of favorable packing of the TTA host by dopant incorporation, which would slow down TTA and is consistent with the longer triplet lifetime at J = 1 mA/cm^2 in **Fig. S9g** [31]. However, the calculated Φ_{TTAUC} by Eq. (2) increased from 15.1% to 37.6% due to higher η_{PLQY} of the emitter layer, and this Φ_{TTAUC} is the recorded-high value in solid state.

4. Conclusions

We have demonstrated that incorporating phosphorescent Ir(ppy)$_3$ into a fluorescent Alq$_3$ matrix creates a dark sensitizer (DS) layer that generates triplets with high efficiency for OLED applications. By using the DS layer, both device efficiency and color performance of blue TTAUC OLEDs were improved relative to fluorescent (Alq$_3$) or phosphorescent (Ir(ppy)$_3$)-sensitized OLEDs. Compared to a conventional blue TTA OLED, DS-TTAUC OLED showed similar color performance but exhibited higher efficiency due to efficient utilization of singlet excitons. The kinetic model and transfer rates were evaluated from TrEL and TRPL data, indicating nearly 100% energy transfer from the Alq$_3$ singlet to its triplet state for 8% Ir(ppy)$_3$ in Alq$_3$. We showed this approach could be extended to other device compositions, suggesting that it can be a general strategy for improving blue OLED performance.

Declaration of Competing Interest

There are no conflicts to declare.

Acknowledgements

This work was supported by the Ministry of Science and Technology (MOST), Taiwan, under Grants MOST 109-2622-E-155-014, 108-2221-E-155-051-MY3, 108-2912-I-155-504, 108-2811-E-155-504-MY3, 107-2221-E-155-058-MY3, 107-2113-M-002-020-MY3, 107-2221-E-002-156-MY3, 107-2221-E-155-027, 107-3113-E-155-001-CC2, 106-3113-E-155-001-CC2, 106-2221-E-155-036, 106-2923-E-155-002-MY3, 106-2923-E-002-004-MY3, 105-2221-E-002-130-MY3, the MEGA project, which has received funding from the European Union's Horizon 2020 research and innovation program under the Marie Skłodowska-Curie grant agreement No 823720. CJB acknowledges support by the National Science Foundation grant CHE-1800187.

Appendix A. Supplementary data

Supplementary data to this article can be found online at https://doi.org/10.1016/j.cej.2021.130889.

References

[1] X. Qiao, D. Ma, Nonlinear optoelectronic processes in organic optoelectronic devices: Triplet-triplet annihilation and singlet fission, Materials Science and Engineering: R: Reports 139 (2020) 100519.
[2] N. Yanai, N. Kimizuka, New triplet sensitization routes for photon upconversion: thermally activated delayed fluorescence molecules, inorganic nanocrystals, and singlet-to-triplet absorption, Acc. Chem. Res. 50 (10) (2017) 2487–2495.
[3] B. Joarder, N. Yanai, N. Kimizuka, Solid-state photon upconversion materials: structural integrity and triplet–singlet dual energy migration, J. Phys. Chem. Lett. 9 (16) (2018) 4613–4624.
[4] T.N. Singh-Rachford, F.N. Castellano, Photon upconversion based on sensitized triplet–triplet annihilation, Coord. Chem. Rev. 254 (21-22) (2010) 2560–2573.
[5] N. Yanai, N. Kimizuka, Recent emergence of photon upconversion based on triplet energy migration in molecular assemblies, Chem. Commun. 52 (31) (2016) 5354–5370.
[6] C. Xiang, C. Peng, Y. Chen, F. So, Origin of Sub-Bandgap Electroluminescence in Organic Light-Emitting Diodes, Small 11 (40) (2015) 5439–5443.
[7] A.K. Pandey, J.-M. Nunzi, Rubrene/Fullerene Heterostructures with a Half-Gap Electroluminescence Threshold and Large Photovoltage, Adv. Mater. 19 (21) (2007) 3613–3617.
[8] C. Fan, W. Wu, J.J. Chruma, J. Zhao, C. Yang, Enhanced Triplet–Triplet Energy Transfer and Upconversion Fluorescence through Host–Guest Complexation, J. Am. Chem. Soc. 138 (47) (2016) 15405–15412.
[9] H. Lai, T. Zhao, Y. Deng, C. Fan, W. Wu, C. Yang, Assembly-enhanced triplet-triplet annihilation upconversion in the aggregation formed by Schiff-base Pt(II) complex grafting-permethyl-β-CD and 9, 10-diphenylanthracence dimer, Chin. Chem. Lett. 30 (11) (2019) 1979–1983.
[10] B.-Y. Lin, C.J. Easley, C.-H. Chen, P.-C. Tseng, M.-Z. Lee, P.-H. Sher, J.-K. Wang, T.-L. Chiu, C.-F. Lin, C.J. Bardeen, J.-H. Lee, Exciplex-Sensitized Triplet–Triplet Annihilation in Heterojunction Organic Thin-Film, ACS Appl. Mater. Interfaces 9 (12) (2017) 10963–10970.
[11] M. Lehnhardt, T. Riedl, T. Rabe, W. Kowalsky, Room temperature lifetime of triplet excitons in fluorescent host/guest systems, Org. Electron. 12 (3) (2011) 486–491.
[12] A. Salehi, C. Dong, D.-H. Shin, L. Zhu, C. Papa, A. Thy Bui, F.N. Castellano, F. So, Realization of high-efficiency fluorescent organic light-emitting diodes with low driving voltage, Nat. Commun. 10 (1) (2019).

[13] G. Vaubel, Intersystem crossing between guest and host molecules in anthracene mixed crystals, Chem. Phys. Lett. 9 (1) (1971) 51–53.
[14] A. Nicolet, M.A. Kol'chenko, B. Kozankiewicz, M. Orrit, Intermolecular intersystem crossing in single-molecule spectroscopy: terrylene in anthracene crystal, J. Chem. Phys. 124(16) (2006) 164711.
[15] G. Vaubel, H. Baessler, Franck-Condon factors in intermolecular intersystem crossing, Chem. Phys. Lett. 11 (5) (1971) 613–616.
[16] J. Lee, C. Jeong, T. Batagoda, C. Coburn, M.E. Thompson, S.R. Forrest, Hot excited state management for long-lived blue phosphorescent organic light-emitting diodes, Nat. Commun. 8 (2017) 15566.
[17] Hyeonghwa Yu, Hany Aziz, Direct Observation of Exciton-Induced Molecular Aggregation in Organic Small-Molecule Electroluminescent Materials, J. Phys. Chem. C 123 (26) (2019) 16424–16429.
[18] Hyeonghwa Yu, Yingjie Zhang, Yong Joo Cho, Hany Aziz, Exciton-Induced Degradation of Carbazole-Based Host Materials and Its Role in the Electroluminescence Spectral Changes in Phosphorescent Organic Light Emitting Devices with Electrical Aging, ACS Appl. Mater. Interfaces 9 (16) (2017) 14145–14152.
[19] N.T. Tierce, C.H. Chen, T.L. Chiu, C.F. Lin, C.J. Bardeen, J.H. Lee, Exciton dynamics in heterojunction thin-film devices based on exciplex-sensitized triplet–triplet annihilation, PCCP 20 (2018) 27449–27455.
[20] Chia-Hsun Chen, Nathan T. Tierce, Man-kit Leung, Tien-Lung Chiu, Chi-Feng Lin, Christopher J. Bardeen, Jiun-Haw Lee, Efficient Triplet–Triplet Annihilation Upconversion in an Electroluminescence Device with a Fluorescent Sensitizer and a Triplet-Diffusion Singlet-Blocking Layer, Adv. Mater. 30 (50) (2018) 1804850.
[21] P.Y. Chou, H.H. Chou, Y.H. Chen, T.H. Su, C.Y. Liao, H.W. Lin, W.C. Lin, H.Y. Yen, I.C. Chen, C.H. Cheng, Efficient delayed fluorescence via triplet–triplet annihilation for deep-blue electroluminescence, Chem. Commun. 50 (2014) 6869–6871.
[22] Kazuma Mase, Keisuke Okumura, Nobuhiro Yanai, Nobuo Kimizuka, Triplet sensitization by perovskite nanocrystals for photon upconversion, Chem. Commun. 53 (59) (2017) 8261–8264.
[23] M.A. Baldo, S. Lamansky, P.E. Burrows, M.E. Thompson, S.R. Forrest, Very high-efficiency green organic light-emitting devices based on electrophosphorescence, Appl. Phys. Lett. 75(1) (1999) 4−6.
[24] Taiju Tsuboi, Woo Sik Jeon, Jang Hyuk Kwon, Observation of phosphorescence from fluorescent organic material Bebq2 using phosphorescent sensitizer, Opt. Mater. 31 (12) (2009) 1755–1758.
[25] Isao Tanaka, Yuichiro Tabata, Shizuo Tokito, Observation of phosphorescence from tris(8-hydroxyquinoline) aluminum thin films using triplet energy transfer from iridium complexes, Phys. Rev. B 71 (20) (2005).
[26] Isao Tanaka, Shizuo Tokito, Phosphorescent-sensitized triplet-triplet annihilation in tris(8-hydroxyquinoline) aluminum, J. Appl. Phys. 97 (11) (2005) 113532.
[27] Isao Tanaka, Yuichiro Tabata, Shizuo Tokito, Förster and Dexter energy-transfer processes in fluorescent BAlq thin films doped with phosphorescent Ir(ppy)3 molecules, J. Appl. Phys. 99 (7) (2006) 073501.
[28] Dawei Di, Le Yang, Johannes M. Richter, Lorenzo Meraldi, Rashid M. Altamimi, Ahmed Y. Alyamani, Dan Credgington, Kevin P. Musselman, Judith L. MacManus-Driscoll, Richard H. Friend, Efficient Triplet Exciton Fusion in Molecularly Doped Polymer Light-Emitting Diodes, Adv. Mater. 29 (13) (2017) 1605987.
[29] Liwen Hu, Guilan Zhang, Yanshan Liu, Ting Guo, Longquan Shao, Lei Ying, Efficient dendrimers based on naphthalene indenofluorene for two-photon fluorescent imaging in living cells and tissues, J. Mater. Chem. C 8 (6) (2020) 2160–2170.
[30] S.J. Cha, N.S. Han, J.K. Song, S.R. Park, Y.M. Jeon, M.C. Suh, Efficient deep blue fluorescent emitter showing high external quantum efficiency, Dyes Pigm. 120 (2015) 200–207.
[31] K. Miyata, F.S. Conrad-Burton, F.L. Geyer, X.Y. Zhu, Triplet pair states in singlet fission, Chem. Rev. 119(6) (2019) 4261−4292.